AAPS PharmSciTech, Vol. 9, No. 1, March 2008 (© 2007)
DOI: 10.1208/s12249-007-9004-x

Research Article

Study of the RESS Process for Producing Beclomethasone-17,21-Dipropionate Particles Suitable for Pulmonary Delivery

Paul A. Charpentier,[1,2] Ming Jia,[1] and Rahima A. Lucky[1]

Received 20 July 2007; accepted 11 September 2007; published online 8 January 2008

Abstract. The purpose of this research was to micronize beclomethasone-17,21-dipropionate (BDP), an anti-inflammatory inhaled corticosteroid commonly used to treat asthma, using the rapid expansion of supercritical solution (RESS) technique. The RESS technique was chosen for its ability to produce both micron particles of high purity for inhalation, and submicron/nano particles as a powder handling aid for use in next generation dry powder inhalers (DPIs). Particle formation experiments were carried out with a capillary RESS system to determine the effect of experimental conditions on the particle size distribution (PSD). The results indicated that the RESS process conditions strongly influenced the particle size and morphology; with the BDP mean particle size decreasing to sub-micron and nanometer dimensions. An increase in the following parameters, i.e. nozzle diameter, BDP mol fraction, system pressure, and system temperature; led to larger particle sizes. Aerodynamic diameters were estimated from the SEM data using three separate relations, which showed that the RESS technique is promising to produce particles suitable for pulmonary delivery.

KEY WORDS: asthma; beclomethasone dipropionate; crystallization; micronization; supercritical fluid processing.

INTRODUCTION

Asthma ranks among one of the most common chronic conditions, affecting over 20 million people in the United States alone, and causing, on an annual basis, over 1.5 million emergency department visits, about 500,000 hospitalizations and 5,500 deaths (U.S. Dept. of health and Human Services, (2002)). Inhaled corticosteroids (ICS), such as beclomethasone dipropionate (BDP), are well-established anti-inflammatory therapies for the treatment of asthma (1), recommended in national treatment guidelines as first-line therapy for this chronic disease (2). The micronization of pharmaceuticals such as BDP with well-defined physical properties and performance characteristics suitable for application in portable inhalers, including next generation dry powder inhalers (DPIs), continues to be a significant challenge for the pharmaceutical industry (3,4). The performance of the DPI strongly depends on both the design of the delivery device and the particulate formulation (5). Currently marketed DPIs provide rather low deposition of drug to the lung (typically below 15%) because of problems with drug retention in the delivery device, combined with non-optimized particle size distribution and particle morphology (6).

Lung deposition of ICS from next generation DPIs could be improved by better control of particle size and morphology (in particular shape) of the active pharmaceutical ingredient (API; 7). Particles of a narrow size distribution with a mass mean aerodynamic diameter (MMAD) in the approximate range from 1–6 μm are desired for the treatment of asthma by inhalation therapy (8). Spherical particles with rough surfaces are generally considered best for pulmonary delivery (9), although elongated particles have been shown to have advantageous aerodynamic behaviour (10). Of additional impetus for this research is a renewed interest in engineering particles for DPI formulation to improve the powder dispersibility for a new generation of DPIs that are being designed for pure API without a carrier, and the use of nanoparticles to act as "lubricants" for increasing powder roughness for accurate dispersing (7,11).

The employment of supercritical fluids (SCFs) has attracted considerable interest as an emerging technology for engineering particles of controlled dimensions (12). Particle formation for pharmaceutical applications using SCFs can be carried out according to several different techniques, each of which has advantages and disadvantages (13). The rapid expansion of supercritical solution process (RESS) is a promising technique to engineer desired particle properties, including submicron and nanoparticles dimensions (14). In the RESS process, the API is dissolved in a high-pressure SCF which is then expanded through a nozzle, where instantaneous nucleation and crystal growth take place at very high supersaturation (15). During the expansion process, the solvent density decreases considerably, causing the API to be ejected from the solution due to low solubility at the gas-like solvent density (16). After the precipitation or crystallization process, the solvent is in the gaseous phase providing solvent free and dry products, hence eliminating extra washing and drying steps. The possibility of obtaining solvent-free, micron and sub-micron particles with a

[1] Department of Chemical and Biochemical Engineering, University of Western Ontario, N6A 5B9, London, Ontario, Canada.
[2] To whom correspondence should be addressed. (e–mail: pcharpentier@eng.uwo.ca

controlled size distribution(s) makes this technique attractive. However, the underlying effects of changing process parameters in the RESS process on controlling particle size and shape are poorly understood. This work explores the RESS process for the production of both micron and submicron/nano particles of the API, BDP, for simultaneous inhalation and powder handling required for next generation DPIs.

EXPERIMENTAL

Materials

The laboratory reagent methanol (HPLC grade, Sigma-Aldrich, Mississauga, Ont.) was used as received. The synthetic steroid beclomethasone 17, 21 dipropionate (BDP), was donated by Glaxo Smithkline (Raleigh, NC), and used as received. This steroid is a member of the glucocorticoid family, a white to creamy white powder, with a molecular mass of 521.25 g/mol and a melting point of 210 °C.

Methods

Solubility

The RESS process requires experimental conditions where the API, in this case BDP, is initially soluble in the SCF before the expansion. The solubility of BDP in methanol and acetone modified supercritical carbon dioxide solutions were elsewhere determined using a phase monitor, and found to form a homogeneous phase under experimental conditions reported here for RESS processing. Of particular interest for this feasibility study was methanol due to its low freezing point (mp=−98 °C), minimizing the effect of cold CO_2 exiting the nozzle on crystal formation, along with having a high volatility in the heated expansion chamber, to leave pure BDP being deposited on the silicon wafer.

RESS Experimental Apparatus and Spraying Procedure

Figure 1 shows the schematic diagram of the experimental apparatus used for RESS processing. The apparatus includes a stainless steel fixed-volume chamber (25 ml) coupled to a capillary nozzle. The extraction vessel was equipped with two quartz windows (Insaco, US) for observation of phase behavior. The vessel was wrapped with heating tape (Omega, USA) to maintain the solution at a desired temperature (±0.2 °C). The internal vessel temperature was measured with a T-type thermocouple (Omega, USA) and controlled with a Fuzzy-Logic controller (Fuji, Mississauga, Ont.). The pressure in the vessel was monitored using a transducer (±1 bar) and a digital display (Omega, USA). The desired amount of BDP and MeOH were added to the extraction vessel to provide the experimental conditions of Table I. The vessel was then heated and pressurized, to the desired set-points. A magnetic stir bar was used to mix the contents of the reactor. The cell also had a rupture disk (HIP, USA) for safety.

A silicon wafer was placed inside a heated precipitation vessel (Parr Instruments, USA) onto which the BDP was sprayed directly. After spraying, the silicon wafer was placed in a sample container to avoid contamination. The average values reported were repeated 2–3× with less than 5% variation being found between repeated experiments.

Four capillary tubes with different internal diameters were tested having a common 1588 micron outer diameter and 3 cm length. The capillary tube (Supelco, Mississauga, Ont.) was held in place by a pressure gland and sleeve (HIP, USA). The volumetric flowrates were measured routinely after cleaning the capillary between experiments to ensure reproducibility. For the nozzle length of 3 cm, the volumetric flow rate of CO_2 at 3,000 and 4,000 psi are 52±3 and 63±3ml/min, respectively.

Characterization

The size and morphology of the precipitates were observed by a scanning electron microscope (SEM, Hitachi S-4500) on gold-sputtered samples of material deposited by the RESS process on silicon wafers. Due to the small amount of material formed in the experiments, particle size distributions were measured by forming histograms of at least 500–1000 particles from SEM photomicrographs using the image analysis

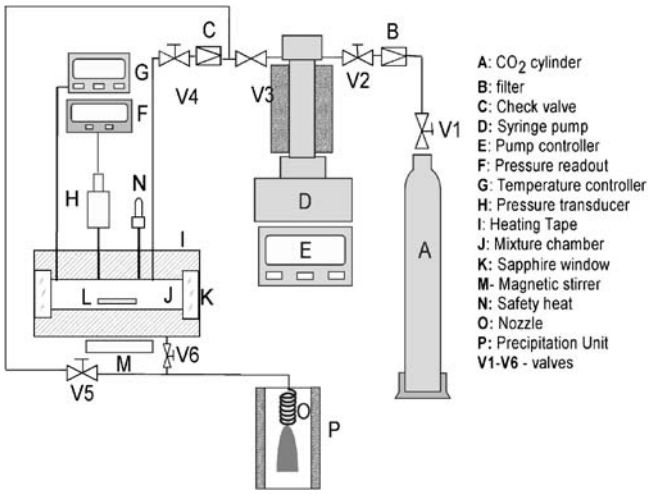

Fig. 1. Rapid expansion of supercritical solution (RESS) experimental apparatus

Table I. RESS Experimental Conditions

Expt. Cond.	T_{mix} (°C)	P_{mix} (psi)	Capillary diameter (μm)	BDP mole fraction
A1	40	3,000	254	2.50×10^{-3}
A2	40	3,000	762	2.50×10^{-3}
A3	40	3,000	1,016	2.50×10^{-3}
B1	43	4,600	127	3.95×10^{-5}
B2	43	4,600	127	6.26×10^{-5}
B3	43	4,600	127	7.81×10^{-5}
B4	43	4,600	127	1.63×10^{-4}
C1	40	1,900	127	8.44×10^{-5}
C2	40	2,500	127	8.44×10^{-5}
C3	40	3,000	127	8.44×10^{-5}
C4	40	4,100	127	8.44×10^{-5}
D1	35	3,000	127	8.44×10^{-5}
D2	40	3,000	127	8.44×10^{-5}
D3	50	3,000	127	8.44×10^{-5}

Methanol concentration=5 mol%, capillary length=3 cm, spray distance is 1 cm

Table II. Experimental Results of BDP Processed by RESS

Exp. Cond.	Mean Diameter (μm)	SD (μm)	Size Range (micron)	Aspect Ratio	Modality[a]
A1	1.01	5.21	0.30–3.15	1.86	U
A2	2.97	11.96	1.10–6.60	4.10	M
A3	9.16	37.06	2.50–18.40	5.33	M
B1	0.24	1.18	0.09–1.10	1.22	U
B2	0.34	1.86	0.11–1.32	1.54	U
B3	0.40	3.44	0.10–2.20	1.79	M
B4	1.94	6.64	0.40–3.90	3.59	M
C1	0.16	1.60	0.02–0.98	1.45	U
C2	0.24	1.11	0.07–1.01	1.40	U
C3	0.34	4.90	0.09–1.48	1.55	M
D1	0.30	4.34	0.07–1.01	1.20	U
D2	0.34	4.90	0.09–1.48	1.55	M
D3	1.28	4.03	0.42–2.73	2.66	M

[a] *U* Unimodal, *M* multimodal

software Scion Image™ (USA). Both the maximum length and aspect ratio were measured and reported in Table II.

Aerodynamic Diameter Measurement

Aerodynamic diameters (D_a) were analyzed by three separate equations using values determined from the electron microscopy results, due to the small amount of material deposited on the Si wafer. The first relation takes into account the influences of both particle density and shape and relates the particle geometric mean diameter (D_p) to D_a by (17):

$$\sqrt{C_a} D_a = D_p \left[\frac{p_p C_p}{\chi p_o} \right]^{1/2} \tag{1}$$

where, C_a and C_p are the Cunningham slip correction factors (close to unity when D_p>1.0 μm), and χ is the dynamic shape factor (unity for spherical particles).

To account for non-spherical particles, the shape factor, χ, was calculated from the SEM data according to Carter and Yan (18):

$$r_{rms,d} = \sqrt{\frac{(r_{max} - r_{mean})^2 + (r_{mean} - r_{min})^2}{2}} \tag{2}$$

$$\text{where } \chi = S_F = \frac{r_{rms,d}}{r_{mean}} \tag{3}$$

The next relation studied uses Cox's theory according to Ku *et al.* (19)

$$D_a = \left(\frac{1}{3} D_{a,\perp} + \frac{2}{3} D_{a,|} \right) \tag{4}$$

where motion perpendicular to the major axis is given by:

$$D_{a,\perp} = D_p \left(\frac{9\rho}{8\rho_w} \{ \ln(2\beta) + 0.193 \} \right)^{\frac{1}{2}} \tag{5}$$

and motion parallel to the major axis is given by:

$$D_{a,||} = D_p \left(\frac{9\rho}{4\rho_w} \{ \ln(2\beta) - 0.807 \} \right)^{\frac{1}{2}} \tag{6}$$

The final equation is empirical and considers fibers according to Martin *et al.* (20):

$$D_a = \frac{3}{2} D_p \sqrt{\frac{\rho/\rho_w}{\frac{0.385}{\ln(2\beta)-0.5} + \frac{1.230}{\ln(2\beta)+0.5}}} \tag{7}$$

where for Eqs. 5, 6, and 7, β is the particle aspect ratio (length/diameter) measured by SEM, ρ is the material density (1.5 g/cc for BDP), and ρ_w is the density of water (1 g/cc).

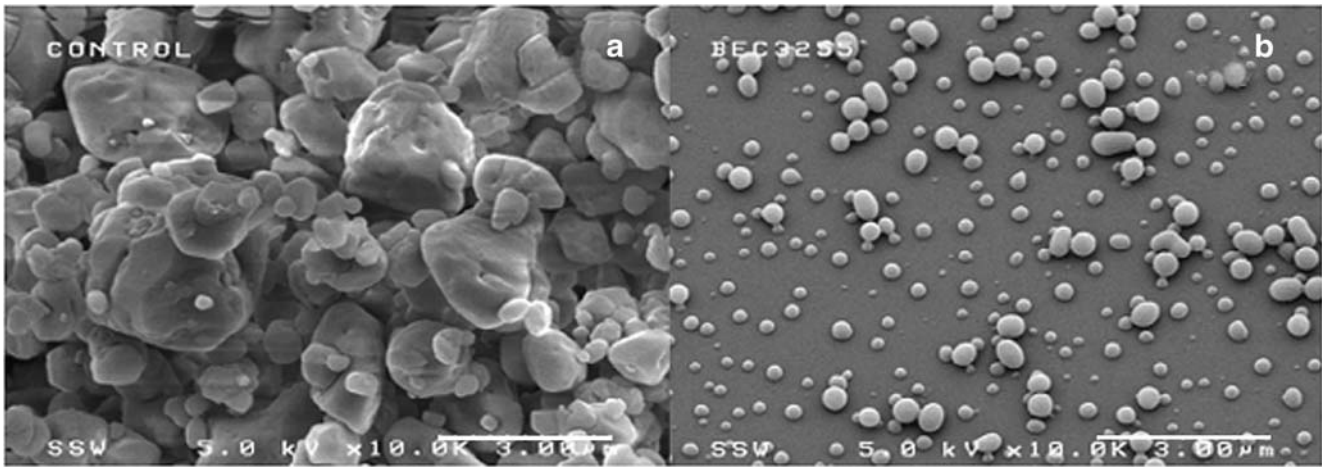

Fig. 2. SEMs of BDP; **a** as received **b** after the RESS process. The experimental conditions were T_{mix}=43 °C, P_{mix}=4,600 psi, Capillary diameter=127 μm, Nozzle length=3 cm, $y_{BDP}=3.95\times10^{-5}$, [MeOH]=5 mol%

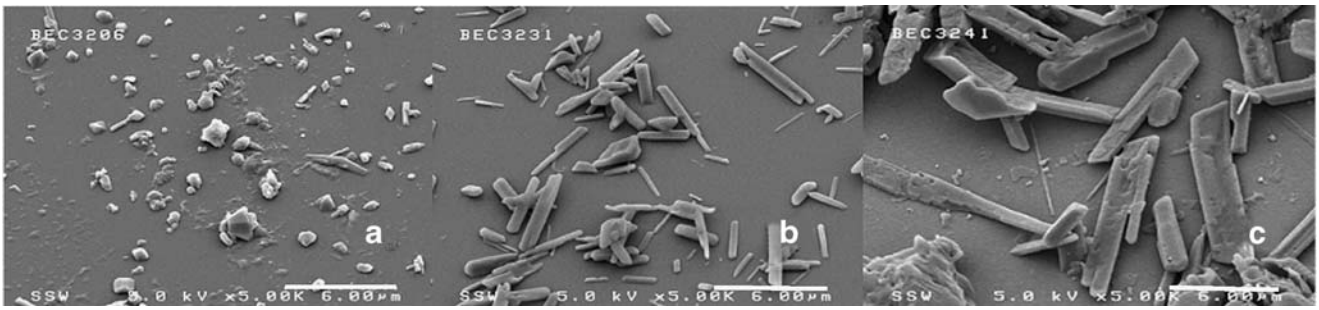

Fig. 3. SEMs of BDP produced by RESS using nozzle diameters of **a** 254 μm, **b** 762 μm, and **c** 1,016 μm. The experimental conditions were T_{mix}=40 °C, P_{mix}=3,000 psi, Nozzle length=3 cm, $y_{BDP}=2.50\times10^{-3}$, [MeOH]=5mol%

RESULTS AND DISCUSSION

Effects of Process Parameters

The SEM photomicrographs of unprocessed and processed BDP are given in Figs. 2a and b. The original BDP particles were small, ranging from 0.4 to 5 μm with irregular particle shape, while RESS processing provided much smaller and more regular particle sizes as shown for a typical experiment in Fig. 2b, where the particle size range was 0.2–1.0 μm. The experimental results in this study showed that much finer particles could be formed with a narrower PSD, as compared to the starting BDP, by using RESS supercritical fluid processing. Our previous work with the GAS process for BDP produced significantly larger and less spherical particles (21). Table I shows the RESS experimental conditions used for studying the following process parameters: A—capillary diameter, B—BDP mole fraction, C—pressure, and D—temperature. Table II shows the results giving the BDP mean diameter, standard deviation, the size range, the aspect ratio, and the modality of BDP particles for the various process parameters, from which we calculate the aerodynamic diameter later to determine potential application for inhalation therapy.

Effect of capillary diameter (A)

Four nozzles of different diameters (127, 254, 762 and 1,016 μm) were studied using the RESS process. When the 127-μm internal diameter nozzle was used for the first set of experimental conditions, significant plugging occurred, so the results are presented for the 3 higher diameter nozzles, as shown in Fig. 3. With increasing nozzle diameter, morphologies of produced BDP particles changed from micron spheres to elongated crystals with increased aspect ratios. Figure 4 provides the particle size distribution curves for the three different nozzle diameters, which shows quantitatively that increasing diameter both increases the mean BDP diameter, and the width of the distribution. As the RESS capillary diameter increased, the BDP D_m and aspect ratio both increased (Table II), which can be explained by the Ostwald step rule for crystallization (22). When $scCO_2$ is depressurized through the capillary into a low-pressure heated chamber, the supercritical solution generates very high supersaturation ratios, and high nucleation rates. The first step for forming a critical nucleus is the formation of a liquid like dense phase or droplet. Beyond a certain critical size, a crystal nucleus forms inside the phase. When the solution jet leaves the larger diameter nozzle, the jet breaks into larger droplets containing more nuclei. Crystals then have a greater chance to collide with one other, agglomerating to form larger particles. Indeed, agglomeration of particles is known to be a key process for particle growth in the RESS process, as mathematical modeling shows particles of less than 20 nm are formed at the tip of a nozzle, which normally grow to much larger sizes (23).

The capillary nozzle was cleaned routinely between experiments to prevent plugging. Although the smaller internal diameter capillary had plugging under these conditions, it was the capillary of choice for future experiments that used lower concentrations of BDP.

Effect of BDP Concentration (B)

The effect of BDP concentration was studied from mol fractions of $3.95–16.3\times10^{-5}$, with Fig. 5 comparing the SEM photomicrographs of BDP produced under these conditions. As seen in this figure and Table II, decreasing the concentration of BDP in $scCO_2$ led to smaller particle sizes and a narrower particle size range. At low concentrations, most of the BDP particles are spherical and relatively unimodal in the submicron size region. There are only a few long crystals observed from SEM micrographs at the mole fraction of 3.95×10^{-5} and 6.26×10^{-5}. When the concentration was increased to the mole fraction of 7.81×10^{-5}, there were more long crystals formed by the RESS process (Fig. 5c). When BDP concentration reached the highest studied mole fraction of 16.3×10^{-5}, the morphology of

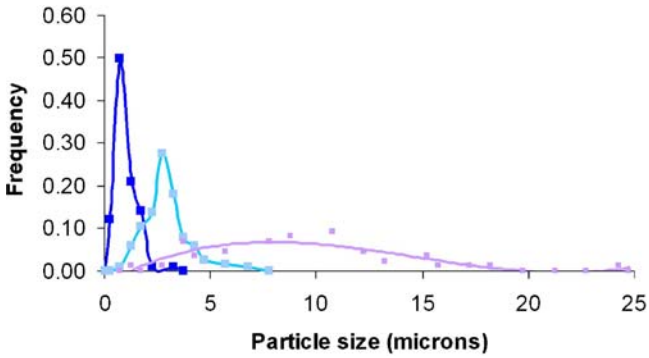

Fig. 4. BDP particle size distributions evaluated at different nozzle diameters: 254 μm (*black squares*), 762 μm (*big gray squares*), and 1016 μm (*small gray squares*). The experimental conditions are the same as in Fig. 3

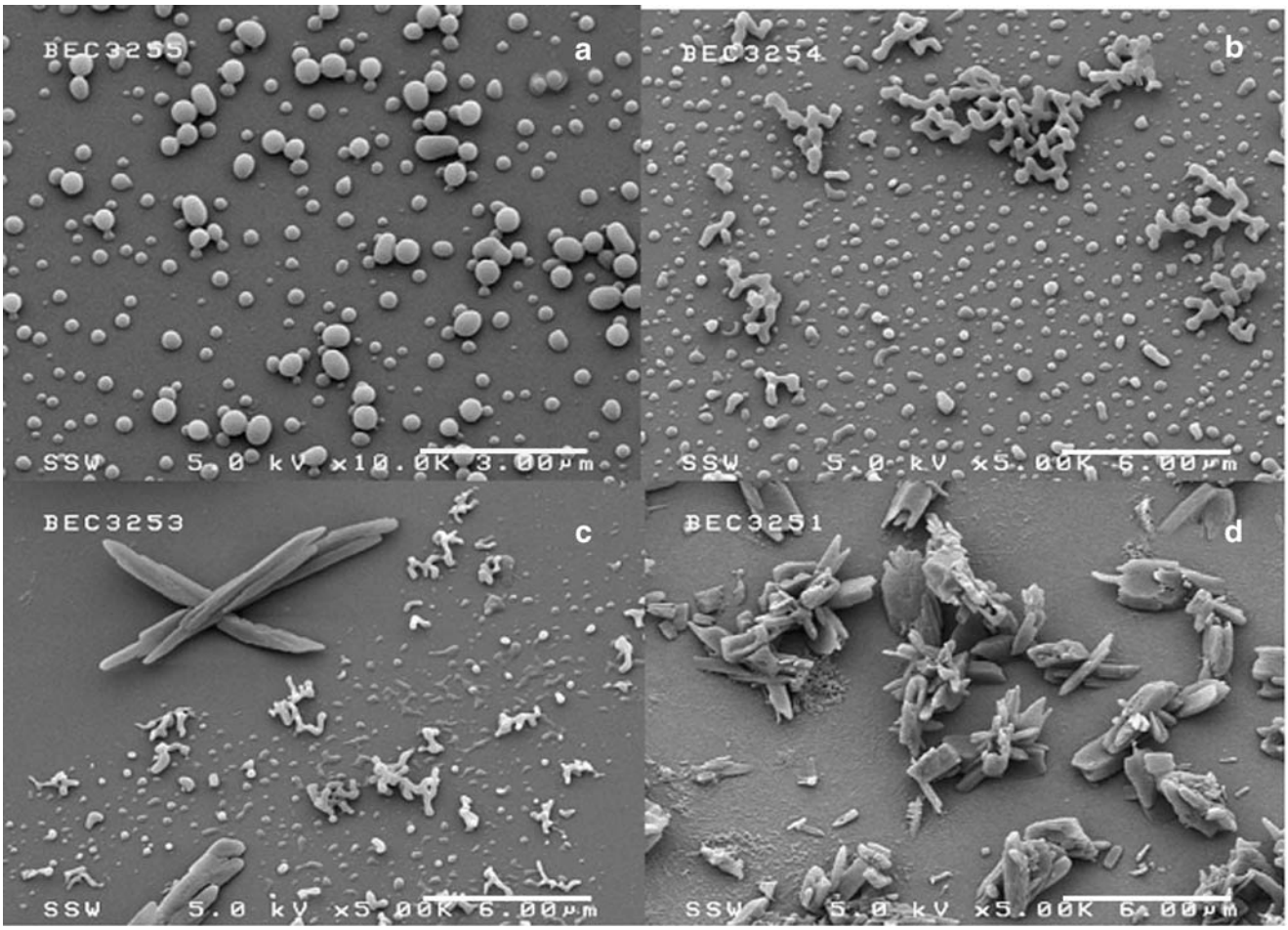

Fig. 5. SEMs of BDP produced by RESS at different mole fractions: **a** 3.95×10^{-5}, **b** 6.26×10^{-5}, **c** 7.81×10^{-5}, **d** 1.63×10^{-4}. The experimental conditions were T_{mix}=43 °C, P_{mix}=4,600 psi, capillary diameter=127 μm, nozzle length=3 cm, [MeOH]=5 mol%

BDP gave long and large crystals, as shown in Fig. 5d. The experimental results showed that as the BDP mol fraction increased, the mean particle diameter and aspect ratio increased. According to the classical theory of nucleation, higher supersaturation ratios produce higher nucleation rates (24). Hence, an increase in the BDP mol fraction leads to a higher supersaturation ratio and should reduce the BDP particle size due to a greater number of nuclei being produced. However, the RESS nozzle used in this work was a capillary, not an orifice. Hence, in addition to the supersaturation ratio, we must also consider particle growth along the length of the capillary due to condensation, coagulation, and agglomeration (25). According to the theory of Lele and Mawson (26) the location of the initial solute condensation along the expansion path determines the particle size and morphology. Sub-micron particles are produced when particles begin to nucleate from the solution phase late in the nozzle, with little time for growth. Larger particles are formed when particles begin to nucleate earlier in the nozzle entrance, and grow very quickly to micron size dimensions. For fiber formation, the precipitation is believed to start upstream of the nozzle entrance, since the solution already has crossed the cloud point. Hence, when the BDP solutions were expanded across the nozzle at the same temperature and pressure, the higher concentration solution would cross the cloud point first, and particle nucleation would begin earlier. The longer path lengths at higher concentrations hence resulted in a larger particle size.

Effect of Pre-Expansion Pressure (C)

An increase of pre-expansion pressure in the range of 1,900–4,100 psi resulted generally in an increase in the particle size and a larger number of long crystals (Fig. 6). At 1,900 psi, the particle size is small with a uniform PSD, and little aggregation (Fig. 6a). At 2,500 psi, the particle size became larger due to the fact that some particles grew and aggregated together, although the formed particles are still unimodal (Fig. 6b). At 3,000 psi, the particle size increased slightly with the aggregation phenomenon becoming obvious, and some long crystals being observed from the SEM photographs. At 4,100 psi, many small spherical particles were formed, along with long crystals. It should be noted that although the original solution temperature was maintained constant before expansion, the capillary was not heated, as it was originally hypothesized that this would minimize agglomeration. The experimental results showed that as the pre-expansion pressure increased, the BDP mean diameter increased, with a slight increase in the aspect ratio. It is not easy to identify a precise trend for expansion pressure from the literature. Turk *et al.* investigated griseofulvin and ß-

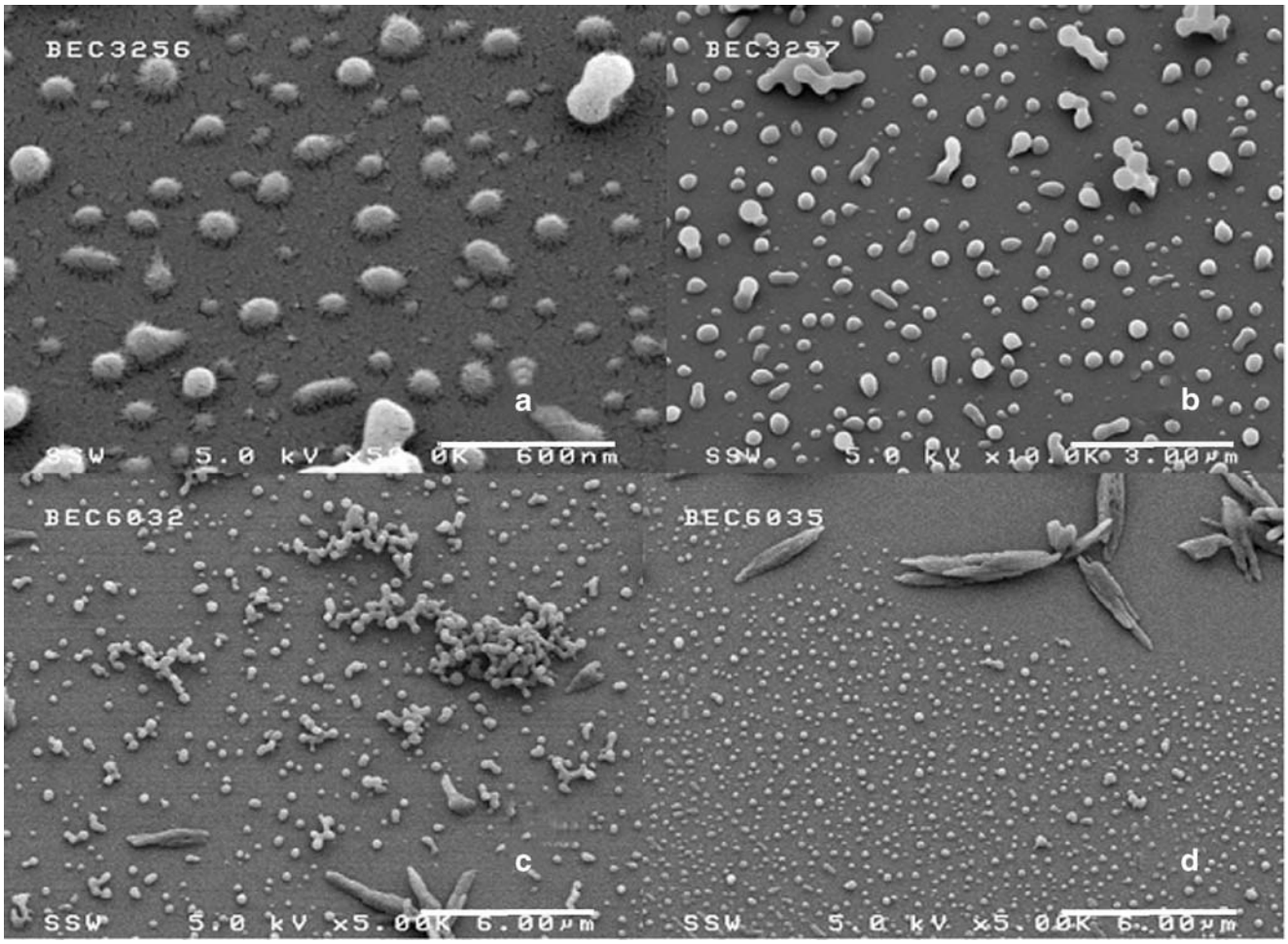

Fig. 6. Effect of pressure on BDP morphology; **a** 1,900 psig, **b** 2,500 psig, **c** 3,000 psig, **d** 4,100 psig. The experimental conditions were T_{mix}=40 °C, capillary diameter=127 μm, nozzle length=3 cm, $y_{BDP}=8.44\times10^{-5}$, [MeOH]=5 mol%

stiosterol with the solvents CO_2 and trifluoromethane, and found that increasing expansion pressure resulted in a decrease of particle size (27). Charoenchaitrakool *et al.* worked with ibuprofen and CO_2 binary system, and found that increasing expansion pressure had no effect on the particle size and morphology (28). Reverchon *et al.* (29). studied salicylic acid in supercritical CO_2, and found that increasing pressure led to an increase of particle size. Experimental tests conducted by Domingo et al. (30) on several materials proved to be inconclusive.

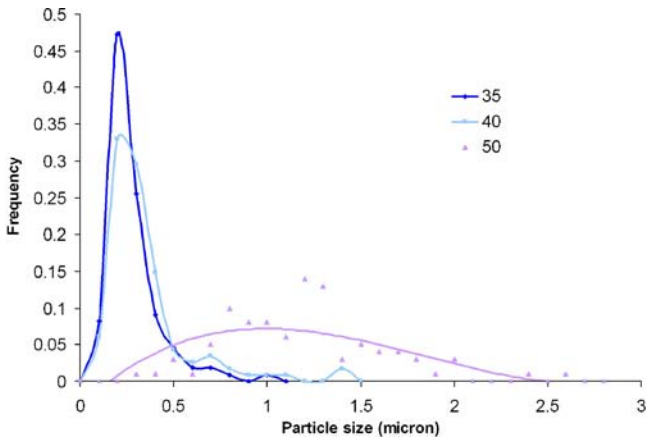

Fig. 7. Effect of temperature on BDP particle size distribution: 35 °C (*diamonds*), 40 °C (*squares*), and 50 °C (*triangles*). The experiment conditions were P_{mix}=3,000 psi, capillary diameter=127 μm, nozzle length=3 cm, $y_{BDP}=8.44\times10^{-5}$, [MeOH]=5 mol%

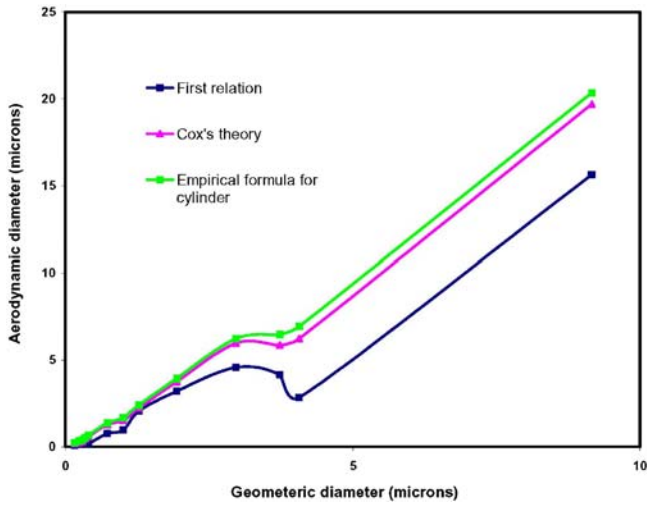

Fig. 8. Aerodynamic diameter *vs* geometric diameter. The points were calculated from the SEM data of Table II according to the equations provided in the Experimental section

Effect of Pre-Expansion Temperature (D)

Results (Table II) and Fig. 7 show that as the pre-expansion temperature increased, the particle size increased from 0.3 μm at 35 °C, to 0.34 at 40 °C, and finally to 1.28 μm microns at 50 °C. At 35 and 40 °C, the curves are essentially unimodal and overlapped; while at 50 °C, the PSD curve becomes very broad. As described in Table II, the morphologies of produced BDP changed from spherical into short stick crystals of higher aspect ratios with increasing pre-expansion temperature.

To explain the effect of increasing pre-expansion temperature increasing the BDP D_m, higher temperature solutions have a higher cloud-point pressure, causing the solutions to cross the cloud point earlier while passing through the capillary, allowing particle nucleation to begin earlier with more time to grow and coalesce. Coagulation and agglomeration are the main reason for producing larger particles in the RESS process, and depend on the rate of successful collision and coalescence. Due to the high melting temperature of the solute compared to the surrounding fluid, growth by condensation is considered to be negligible (31). In high temperatures, the rate of coalescence is faster than collision, and collisions of particles result in coagulated particles (32).

Aerodynamic Diameter

Figure 8 shows the aerodynamic diameter of particles as a function of the geometric diameter (i.e. mean diameter measured by SEM and provided in Table II). For BDP particles with small geometric diameters up to 2 μm, which were normally spherical, the aerodynamic diameters calculated from the three different relations are reasonably similar. However, the first equation breaks down for particle sizes larger than 2 μm, (often nonspherical), as it uses a shape factor which cannot be accurately calculated from the SEM based data. The second and third relations consider the aspect ratio for the nonspherical fibers, and provide very similar results for the BDP system under analysis. The second relation (Eq. 4) is based on Cox's theory and shown to work for carbon nanotubes in the 100–700 nm range (19). It is well known that inhaled spherical particles larger than 5 um are known to be deposited in the mouth, throat, and upper airways, but interestingly fibers as long as 100 um with micron or submicron diameters can reach the gas-exchange regions of the lung, hence being of potential interest for inhalation therapy (33).

The results in this work indicate that the aerodynamic diameter of the produced BDP is within the range of ca 0.2–7 μm with potential application for engineering particles for inhalation studies. Future studies will learn how to optimize the PSDs for next generation DPIs using supercritical fluid processing using a combination of approaches for tuning particle size distributions, and how submicron/nanoparticles affect the powder dispensing.

CONCLUSIONS

The rapid expansion of supercritical solutions (RESS) process was found to be a promising method to form small and monodisperse particles. After the RESS process, the BDP mean particle size decreased to sub-micron and nanometer dimensions. Controlled growth of particles is possible by selecting experimental conditions in such a way that particles begin to nucleate at the nozzle exit with little time to grow. An increase in the following parameters, i.e. nozzle diameter, BDP mol fraction, system pressure, and system temperature; led to larger particle sizes.

ACKNOWLEDGEMENTS

The authors thank Dr. J. P. Mitchell of Trudell Medical International for the fruitful discussions during this work, Dr. Michiel Van Oort of GlaxoSmithKline, and Mr. Brad Kobe of Surface Science Western for use of the Scanning Electron Microscope. This work was financially supported by the Canadian Natural Science and Engineering Research Council (NSERC) and by the University of Western Ontario Academic Development Fund.

REFERENCES

1. P. J. Barnes, S. Pedersen, and W. W. Busse. Efficacy and safety of inhaled corticosteroids. New developments. Am J Respir Crit Care Med. 157(3):1–53 (1998).
2. National Asthma Education and Prevention Program. Expert Panel Report: Guidelines for the Diagnosis and Management of Asthma, Update on Selected Topics 2002. Bethesda, MD. (2003).
3. H. S. Tan, and S. Borsadia. Particle formation using supercritical fluids: Pharmaceutical applications. Exp Opin Ther Patents. 11 (5):861–872 (2001).
4. A. H. L. Chow, H. Y. Tong, P. Chattopadhyay, and B. Y. Shekunov. Particle engineering for pulmonary drug delivery. Pharm Res. 24(3):411–437 (2007).
5. N. Chew, and H.-K. Chan. Use of solid corrugated particles to enhance powder aerosol performance. Pharm Res. 18(11):1570 (2001).
6. M. P. Timsina, G. P. Martin, C. Marriott, D. Ganderton, and M. Yianneskis. Drug delivery to the respiratory tract using dry powder inhalers. Int J Pharm. 101(1):1–13 (1994).
7. H.-K. Chan, P. M. Young, D. Traini, and M. Coates. Dry powder inhalers: challenges and goals for next generation therapies. Pharmaceutical Technology Europe. 19(4):19–24 (2007).
8. M. B. M. N. Dolovich, P. J. Anderson, C. A. Carmargo, N. Chew, C. H. Cole, R. Dhand, J. B. Fink, N. J. Gross, D. R. Hess, A. J. Hickey, C. S. Kim, T. B. Martonen, D. J. Pierson, B. K. Rubin, and G. C. Smaldone. Consensus statement: Aerosols and delivery devices. *Respir Care* **45**:589–596 (2000).
9. P. M. Young, D. Traini, M. Coates, and H. K. Chang. Recent advances in understanding the influence of composite-formulation properties on the performance of dry powder inhalers. *Physica B* **394**:315–319 (2007).
10. H. K. Chan and I. Gonda. Physicochemical characterization of a new respirable form of nedocromil. *J Pharm Sci* **84**:692–696 (1995).
11. J. G. Weers, T. E. Tarara, and A. R. Clark. Design of fine particles for pulmonary drug delivery. Expert Opin Drug Deliv. 4 (3):297–313 (2007).
12. I. Pasquali, R. Bettini, and F. Giordano. Solid-state chemistry and particle engineering with supercritical fluids in pharmaceutics. *Eur J of Pharm Sci* **27**:299–310 (2006).
13. C. Vemavarapua, M. J. Mollana, M. Lodayaa, and T. E. Needhamb. Design and process aspects of laboratory scale SCF particle formation systems. Int J Pharm. 292(1–2):1–16 (2005).
14. X. Ye, and C. M. Wai. Making nanomaterials in supercritical fluids: A review. J Chem Ed. 80(2):198–203 (2003).
15. C. Y. Tai, and C.-S. CHeng. Effect of CO2 on expansion and supersaturation of saturated solutions. AIChE J. 44(4):989–992 (1998).

16. R. K. Franklin, J. R. Edwards, Y. Chernyak, R. D. Gould, F. Henon, and R. G. Carbonell. Formation of perfluoropolyether coatings by the rapid expansion of supercritical solutions (RESS) process. Part 2: Numerical modeling. Ind Eng Chem Res. 40 (26):6127–6139 (2001).
17. W. C. Hinds. *Properties, Behavior, and Measurement of Airborne Particles, Second Edition*, Wiley-Interscience, N.Y., USA, 1999.
18. R. M. Carter and Y. Yan. Measurement of particle shape using digital imaging techniques. *J Phys Conf Ser* **15**:177–182 (2005).
19. B. K. Ku, M. S. Emergy, A. D. Maynard, M. R. Stolzenburg, and P. H. McMurry. In situ structure characterization of airborne carbon nanofibres by a tandem mobility-mass analysis. *Nanotechnology* **17**:3613–3621 (2006).
20. A. R. Martin, W. H. Finlay, M. J. Brett, and D. Vick. Generation and Recovery of Sub-Micron Diameter Fibrous Aerosols. Proceedings of the 2005 International Conference on MEMS, NANO, and Smart Systems. (2005).
21. Y. Bakhbakhi, P. A. Charpentier, and S. Rohani. Experimental study of the GAS process for producing microparticles of beclomethasone-17,21-dipropionate suitable for pulmonary delivery. Int J Pharm. 309(1–2):71 (2006).
22. A. Cacciuto, S. Auer, and D. Frenkel. Onset of heterogeneous crystal nucleation in colloidal suspensions. *Nature* **428**:404–406 (2004).
23. B. Helfgen, M. Turk, and K. Schaber. Hydrodynamic and aerosol modelling of the rapid expansion of supercritical solutions (RESS-process). J Supercrit Fluids. 26(3):225 (2003).
24. D. W. Matson, J. L. Fulton, R. C. Petersen, and R. D. Smith. Rapid Expansion of Supercritical Fluid Solution: Solute Formation of Powders, Thin Films and Fibers. *Ind Eng Chem Res* **26**:2298–2306 (1987).
25. P. G. Debenedetti, J. W. Tom, X. Kwauk, and S.-D. Yeo. Rapid expansion of supercritical solutions (RESS): Fundamentals and applications. *Fluid Phase Equilib* **82**:311–321 (1993).
26. S. Mawson, K. P. Johnston, J. R. Combes, and J. M. DeSimone. Formation of poly(1,1,2,2-tetrahydroperfluorodecyl acrylate) submicron fibers and particles from supercritical carbon dioxide solutions. *Macromolecules* **28**:3182–3191 (1995).
27. M. Turk, B. Helfgen, P. Hils, R. Lietzow, and K. Schaber. Micronization of pharmaceutical substances by rapid expansion of supercritical solutions (RESS): experiments and modeling. *Part Part Syst Charact* **19**:327–335 (2002).
28. M. Charoenchaitrakool, F. Dehghani, N. R. Foster, and H. K. Chan. Micronization by rapid expansion of supercritical solutions to enhance the dissolution rates of poorly water-soluble pharmaceuticals. Ind Eng Chem Res. 39(12):4794–4802 (2000).
29. E. Reverchon, G. Donsi, and D. Gorgoglione. Salicylic acid solubilization in supercritical CO_2 and its micronization by RESS. *J Supercrit Fluids* **6**:241–248 (1993).
30. C. Domingo, E. Berends, and G. M. Van Rosmalen. Precipitation of ultrafine organic crystals from the rapid expansion of supercritical solutions over a capillary and a frit nozzle. J Supercrit Fluids. 10:35–55 (1997).
31. A. Sane, and M. C. Thies. The formation of fluorinated tetraphenylporphyrin nanoparticles via rapid expansion processes: RESS *vs* RESOLV. J Phys Chem B. 109(42):19688–19695 (2005). October 27, 2005
32. T. Hawa, and M. R. Zachariah. Coalescence kinetics of unequal sized nanoparticles. J Aerosol Sci. 37(1):1 (2006).
33. H. Larhrib, G. P. Martin, C. Marriott, and D. Prime. The influence of carrier and drug morphology on drug delivery from dry powder formulations. Int J Pharm. 257:283–296 (2003).